help design field blocking and beam arrangements, if X-ray simulation is used (4,6). However, contrast may not be needed to determine the position of the prostate when CT simulation is performed. In this survey, there were no questionnaires on the usage of magnetic resonance imaging (MRI) images for prostate cancer treatment planning. Going forward, it is expected that MRI/CT image fusion techniques will be increasingly important to define the anatomical structures including the prostate (7,8). The next PCS survey will take this issue into consideration.

Regular or multiple verifications of the treatment fields were performed in only 30% of the patients in this study. In the USA, radiation fields were verified with regular intervals in 60% of the prostate patients surveyed in the 1989 PCS (4). It is hoped that if electric portal imaging devices become more popular in Japan, verification of the treatment fields will be performed more frequently.

Simulations and treatments were performed in the supine position in almost all patients. Published literature suggests a variation in results between the use of the prone and supine positions for prostate cancer radiotherapy. Several authors demonstrated that the rectal dose was reduced in the prone position (9,10). However, in the absence of immobilization devices, daily setup reproducibility may be less accurate for the prone position, primarily due to systematic setup variations (10). Patient positioning procedures in prostate radiotherapy should be evaluated in each institution, in particular if the radiation doses to the prostate are high.

Immobilization was used in only 15% of the patients. This may be in part because immobilization devices for body malignancies are not covered by health insurance in Japan. As mentioned above, patient immobilization can be an important contributor to the reproducibility and accuracy of radiotherapy (11). More widespread use of immobilization devices will also be required with an increase in treatment using 3DCRT or IMRT, which utilize higher dosages of radiation.

The radiation doses delivered to the prostate were affected by the leaf width of MLC. However, there were no significant differences between a 5 mm and a 10 mm MLC leaf size. Leal et al. (12) showed that the impact on the clinical dose distribution due to the MLC leaf width change from 10 to 5 mm is quite low on the dose distribution in patients treated with 3DCRT and IMRT. On the other hand, Wang et al. (13) insisted that the use of the micro-MLC for IMRT of the prostate resulted in significant improvement in the dose distributions to the prostate and critical organs. Although narrower leaves give better sparing of organs at risks, the clinical value should be carefully evaluated.

Several significant variances in the process according to the stratification of institutions were also observed. Although CT data were used for planning in ~90% of the patients, 3D conformal techniques including IMRT were applied less frequently in B institutions. In particular, only 37.5% of the patients were treated with 3D conformal techniques in B2 institutions. In B institutions, lower photon energies <10 MV were also used more frequently. Delivery of high radiation doses without the use of 3D conformal techniques may produce late morbidity of the surrounding tissues. Because some guidelines have recommended that 3DCRT or IMRT techniques should be employed in external beam radiotherapy for prostate cancer (14,15), structural improvement in B institutions should be urgently considered.

In conclusion, the results of the survey identified the standard of practice for treatment planning of prostate cancer in Japan. Although the preferred methods of planning and delivery have been defined somewhat differently at various institutions, it is necessary to define and develop recommended guidelines for the treatment planning process, in particular, for a clinical trial on radiotherapy for prostate cancer.

Acknowledgements

We thank all radiation oncologists who participated in this study. Their efforts at providing us with the necessary information make these surveys possible.

Funding

This study was supported by the Grant-in Aid for Cancer Research (No. 18-4) from the Ministry of Health, Labor and Welfare.

Conflict of interest statement

None declared.

References

1. Nakamura K, Ogawa K, Yamamoto T, Sasaki T, Koizumi M, Teshima T, et al. Trends in the practice of radiotherapy for localized prostate cancer in Japan: a preliminary patterns of care study report. *Jpn J Clin Oncol* 2003;33:527–32.
2. Ogawa K, Nakamura K, Onishi H, Sasaki T, Koizumi M, Shioyama Y, et al. Radical external beam radiotherapy for clinically localized prostate cancer in Japan: differences in the patterns of care between Japan and the United States. *Anticancer Res* 2006;26:575–80.
3. Teshima T, Japanese PCS Working Group. Patterns of care study in Japan. *Jpn J Clin Oncol* 2005;35:497–506.
4. Gerber RL, Smith AR, Owen J, Hanlon A, Wallace M, Hanks G. Patterns of care survey results: treatment planning for carcinoma of the prostate. *Int J Radiat Oncol Biol Phys* 1995;33:803–8.
5. Ogawa K, Nakamura K, Onishi H, Koizumi M, Sasaki T, Araya M, et al., Japanese Patterns of Care Study Working Subgroup of Prostate Cancer. Influence of age on the pattern and outcome of external beam radiotherapy for clinically localized prostate cancer. *Anticancer Res* 2006;26:1319–25.
6. Valicenti RK, Sweet JW, Hauck WW, Hudes RS, Lee T, Dicker AP, et al. Variation of clinical target volume definition in three-dimensional conformal radiation therapy for prostate cancer. *Int J Radiat Oncol Biol Phys* 1999;44:931–5.
7. Roach M, 3rd, Faillace-Akazawa P, Malfatti C, Holland J, Hricak H. Prostate volumes defined by magnetic resonance imaging and computerized tomographic scans for three-dimensional conformal radiotherapy. *Int J Radiat Oncol Biol Phys* 1996;35:1011–8.

8. Nakamura K, Shioyama Y, Tokumaru S, Hayashi N, Oya N, Hiraki Y, et al. Variation of clinical target volume definition among Japanese radiation oncologists in external beam radiotherapy for prostate cancer. *Jpn J Clin Oncol* 2008;38:275–80.
9. O'Neill L, Armstrong J, Buckney S, Assiri M, Cannon M, Holmberg O. A phase II trial for the optimisation of treatment position in the radiation therapy of prostate cancer. *Radiother Oncol* 2008;88:61–6.
10. Weber DC, Nouet P, Rouzaud M, Miralbell R. Patient positioning in prostate radiotherapy: is prone better than supine? *Int J Radiat Oncol Biol Phys* 2000;47:365–71.
11. Fiorino C, Reni M, Bolognesi A, Bonini A, Cattaneo GM, Calandrino R. Set-up error in supine-positioned patients immobilized with two different modalities during conformal radiotherapy of prostate cancer. *Radiother Oncol* 1998;49:133–41.
12. Leal A, Sánchez-Doblado F, Arráns R, Capote R, Lagares JI, Pavón EC, et al. MLC leaf width impact on the clinical dose distribution: a Monte Carlo approach. *Int J Radiat Oncol Biol Phys* 2004;59: 1548–59.
13. Wang L, Hoban P, Paskalev K, Yang J, Li J, Chen L, et al. Dosimetric advantage and clinical implication of a micro-multileaf collimator in the treatment of prostate with intensity-modulated radiotherapy. *Med Dosim* 2005;30:97–103.
14. Jereczek-Fossa BA, Orecchia R. Evidence-based radiation oncology: definitive, adjuvant and salvage radiotherapy for non-metastatic prostate cancer. *Radiother Oncol* 2007;84:197–215.
15. National Comprehensive Cancer Network. NCCN Clinical Practice Guidelines in Oncology: Prostate Cancer V2. 2009. http://www.nccn.org/.

Radiotherapy and Oncology 90 (2009) 422–423

Contents lists available at ScienceDirect

Radiotherapy and Oncology

journal homepage: www.thegreenjournal.com

Letter to the Editor

First clinical cone-beam CT imaging during volumetric modulated arc therapy

To the Editor

Tumor registration using on-board cone-beam CT (CBCT) prior to radiotherapy has been increasingly adopted for daily clinical practice, and it is assumed that the tumor remains still during the treatment. We reported the first clinical kilovoltage (kV) CBCT imaging during rotational radiotherapy using a linac with a CBCT unit (Elekta Synergy, Crawley, UK) [1], wherein a future application to intensity modulated arc therapy (IMAT) [2] was proposed. The effect on CBCT image quality during rotational treatments was first reported in ESTRO conference in 2004 [3]. The purpose of in-treatment CBCT imaging is the direct verification of time-averaged tumor position during treatment. With a latest linac control software, a more advanced IMAT, namely volumetric modulated arc therapy (VMAT), became clinically feasible [4]. In this letter, we present the first clinical CBCT imaging during VMAT delivery using Elekta Synergy. As was described in our previous report [1], the current Synergy system does not allow simultaneous delivery of kV CBCT beams and MV rotational beams. A method for disabling this interlock was therefore investigated, and it was deactivated with the first author's responsibility.

A treatment planning system, ERGO++ 1.7.1 (Elekta 3DLine, Milano), was employed to make a VMAT plan for a prostate cancer patient. A single arc consisting of 73 fixed beams was defined with 5° spacing. The MLC field shape in each beam's eye view was determined by conformal strategy if rectum is located behind the target, whereas the field shape was determined by conformal avoidance strategy if rectum lies in front of the target. Subsequently, each radiation intensity or monitor unit (MU) was optimized by simulated annealing algorithm with a cost function formulated by given physical dose constraints. Then, the resulting MUs were transferred to the linac.

Tumor registration was performed between a planning CT image and a CBCT image immediately after patient set-up. The registration was done by a built-in bone-matching algorithm. The patient couch was adjusted according to the registration results, and then the CBCT imaging was repeated three times: immediately before treatment, during VMAT delivery, and immediately after treatment.

The linac photon energy was 6 MV. For a record and verify system, Mosaiq 1.41 beta (Elekta IMPAC, USA) was employed. A linac control software, Desktop Pro R.7.0, was used. A single-arc VMAT required approximately 3 min and 20 s, which also equals the CBCT projection data acquisition time. The number of projection images was 1222, and the resulting imaging dose at the center of an acrylic phantom having a diameter of 30 cm was approximately 3 cGy.

The figures show axial CBCT images (a) immediately before treatment after registration, (b) during VMAT delivery, and (c) immediately after treatment (Fig. 1). It was confirmed that the tumor position was well maintained. During VMAT beam delivery, the dose rate and the gantry speed are dynamically adjusted [4] according to the calculated MU for each gantry angle. In the present case, the gantry speeds ranged from 0 to 4°/s with a mean of 1.78°/s and a standard deviation of 0.56°/s. A major concern was whether this non-constant gantry speed would generate significant image artifacts. So far we have evaluated several images of phantoms and a prostate cancer patient. No major image artifacts have been detected that may affect the tumor position verification.

In conclusion, the tumor position during VMAT delivery was clinically verified for the first time using kV CBCT. Future work

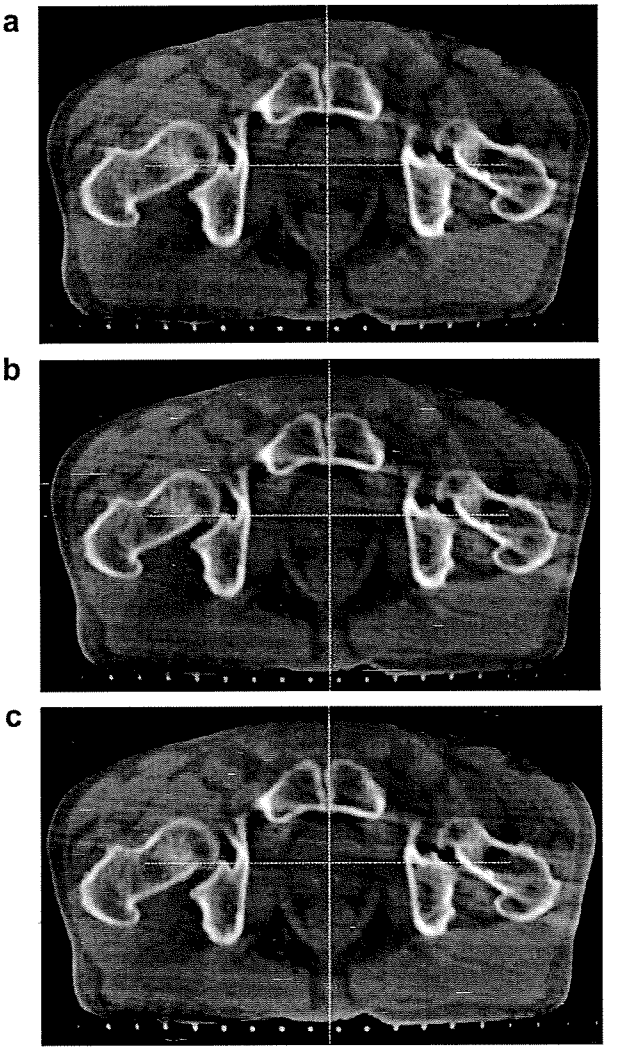

Fig. 1. kV CBCT axial images of a prostate cancer patient: (a) immediately before treatment after registration, (b) during VMAT delivery, and (c) immediately after treatment. The cross lines indicate the isocenter.

0167-8140/$ - see front matter
doi:10.1016/j.radonc.2008.11.009

includes further investigation regarding the effects of the non-constant gantry speed during CBCT image acquisition. Our previous report [1] showed that the CBCT image quality was not visually degraded up to a treatment field size of 10×10 cm^2. More quantitative analysis may be required for VMAT with larger field sizes. Lastly, in-treatment CBCT images may be useful in decision making for subsequent treatment margin or dose adjustment.

References

[1] Nakagawa K, Yamashita H, Shiraishi K, Igaki H, Terahara A, Nakamura N, et al. Verification of in-treatment tumor position using kilovoltage cone-beam computed tomography: a preliminary study. Int J Radiat Oncol Biol Phys. 2007;69:970–3.
[2] Yu CX. Intensity-modulated arc therapy with dynamic multileaf collimation: an alternative to tomotherapy. Phys Med Biol 1995;40:1435–49.
[3] Williams P, Sykes J, Moore C J. The effects of radiation scatter from simultaneous MV irradiation on kV fluoroscopic and X-ray volume imaging with the Elekta Synergy system, ESTRO, Amsterdam 2004. Radiother Oncol 2004;73(Suppl. 1).
[4] Bedford JL, Nordmark HV, McNair HA, Aitken AH, Brock JE, Warrington AP. Treatment of lung cancer using volumetric modulated arc therapy and image guidance. A case study. Acta Oncol 2008;47:1438–43

Keiichi Nakagawa *,
Akihiro Haga,
Kenshiro Shiraishi,
Hideomi Yamashita,
Hiroshi Igaki,
Atsuro Terahara,
Kuni Ohtomo,
Shigeki Saegusa,
Takashi Shiraki,
Takashi Oritate
Department of Radiology,
University of Tokyo Hospital,
Tokyo, Japan
E-mail address: k-nak@fg7.so-net.ne.jp (K. Nakagawa)

Kiyoshi Yoda
Elekta, KK, 6-1-9 Isogami-dori,
Chuo-ku, Kobe, Japan

* Corresponding author.

Acknowledgements

This study was financially supported by the Finnish Breast Cancer Group, Kuopio University, and Kuopio University Hospital. I declare that I have no conflict of interest.

References

[1] Hirvikoski PP, Kumpulainen EJ, Johansson RT. CNF combination as adjuvant treatment in breast cancer patients is well tolerated. Anti-Cancer Drugs 1997;8:376–8.
[2] Hirvikoski PP, Kumpulainen EJ, Johansson RT. Hepatic toxicity caused by adjuvant CMF/CNF in breast cancer patients and reversal by tamoxifen. Breast Cancer Res Treat 1997;44:269–74.
[3] Kumpulainen EJ, Hirvikoski PP, Pukkala E, Johansson RT. Cancer risk after adjuvant chemo- or chemohormonal therapy of breast cancer. Anti-Cancer Drugs 1998;9:131–4.
[4] Bonadonna G, Valagussa P. Dose-response effect of adjuvant chemotherapy in breast cancer. N Engl J Med 1981;304: 10–5.
[5] Saarto T, Blomqvist C, Rissanen P, Auvinen A, Elomaa I. Haematological toxicity: A marker of adjuvant chemotherapy efficacy in stage II and III breast cancer. Br J Cancer 1997; 75:301–5.
[6] Poikonen P, Saarto T, Lundin J, Joensuu H, Blomqvist C. Leucocyte nadir as a marker for chemotherapy efficacy in node-positive breast cancer treated with adjuvant CMF. Br J Cancer 1999;80:1763–6.
[7] Mayers C, Panzarella T, Tannock IF. Analysis of the prognostic effects of inclusion in a clinical trial and of myelosuppression on survival after adjuvant chemotherapy for breast carcinoma. Cancer 2001;91:2246–57.
[8] Bergh J, Wiklund T, Erikstein B, Lidbrink E, Lindmar H, Malmström P, et al. Tailored fluorouracil, epirubicin, and cyclophosphamide compared with marrow-supported high-dose chemotherapy as adjuvant treatment for high-risk breast cancer: A randomised trial. Scandinavian Breast Group 9401 study. Lancet 2000;356:1384–91.

First report on prostate displacements immediately before and after treatment relative to the position during VMAT delivery

KEIICHI NAKAGAWA[1]*, KENSHIRO SHIRAISHI[1]*, SATOSHI KIDA[1], AKIHIRO HAGA[1], KENTARO YAMAMOTO[1], SHIGEKI SAEGUSA[1], ATSURO TERAHARA[1], SAORI ITOH[1], KUNI OHTOMO[1] & KIYOSHI YODA[2]

[1]*Department of Radiology, University of Tokyo Hospital, 7-3-1 Hongo Bunkyo-ku Tokyo 113-8655 Japan and* [2]*Elekta KK, Kobe, Japan*

To the Editor

Previously we reported the first clinical kilovoltage (kV) cone-beam CT (CBCT) imaging during volumetric modulated arc therapy (VMAT) using a linac with an on-board CBCT unit (Elekta Synergy, Crawley, UK) [1], The effect on CBCT image quality during rotational treatments was first presented in ESTRO conference in 2004 [2] and the first clinical in-treatment CBCT images were acquired for rotational lung treatment [3]. The purpose of in-treatment CBCT imaging is direct verification of time-averaged tumor position during treatment. Reported standard deviation of intrafraction prostate movements for 20 patients during 10 fractions was 1.4 mm in cranio-caudal direction [4], which may support the validity of the time-averaged CBCT images. In this letter, prostate displacements immediately before and after treatment relative to the position during VMAT delivery have been reported for the first time. As was described in our previous articles [1,3], the current Synergy system does not allow simultaneous delivery of kV CBCT beams and MV rotational beams. A method for disabling this interlock was therefore investigated and it was deactivated with the first author's responsibility.

A treatment planning system, ERGO++ 1.7.1 (Elekta 3DLine, Milano) was employed to create a VMAT plan for a prostate cancer patient. A single arc consisting of 73 fixed beams was defined with 5 degree spacing. More detailed VMAT delivery and CBCT procedures were described in our previous article [1].

* Equal contributors.

Correspondence: Keiichi Nakagawa, Department of Radiology, University of Tokyo Hospital, 7-3-1 Hongo Bunkyo-ku, Tokyo 113-8655, Japan.

(Received 24 May 2009; accepted 6 June 2009)

34-186X print/ISSN 1651-226X online © 2009 Informa UK Ltd. (Informa Healthcare, Taylor & Francis AS)
3109/02841860903101190

Tumor registration was performed between a planning CT image and a CBCT image immediately after patient set-up. CBCT imaging was conducted four times a day once a week for six weeks; the timings were before couch adjustment, after couch adjustment, during VMAT delivery, and immediately after the treatment. The couch adjustment was done by automatic bone matching between planning CT and the CBCT images followed by manual operation based on calcification inside the prostate organ. Subsequently, off-line image registration was performed between two CBCT images of the same day to evaluate prostate displacements using the above mentioned matching procedures.

Figure 1 shows CBCT prostate images of a particular day for a patient with calcification inside the prostate organ. Images in the first row were acquired immediately before VMAT treatment after couch adjustment, the second row refers to images during VMAT delivery, and the third row images were taken immediately after the treatment. Crossing lines indicate the isocenter.

The mean and standard deviation of displacements at the time of pre-treatment against the in-treatment position of all the six days for the patient were 0.1 ± 0.2 mm, -0.3 ± 0.4 mm, and -0.4 ± 0.6mm in lateral, vertical, and longitudinal directions. The mean and standard deviation of displacements at the time of post-treatment against the in-treatment position of all the six days for the same patient were 0.2 ± 0.3 mm, -0.8 ± 0.7 mm, and -0.3 ± 0.6 mm in lateral, vertical, and longitudinal directions. No statistical conclusion can be drawn using the present limited data sets.

In conclusion, displacements of the prostate gland immediately before and after treatment relative to the position during VMAT delivery were reported for the first time using kV CBCT, which may facilitate decision making for subsequent treatment margin or dose adjustment.

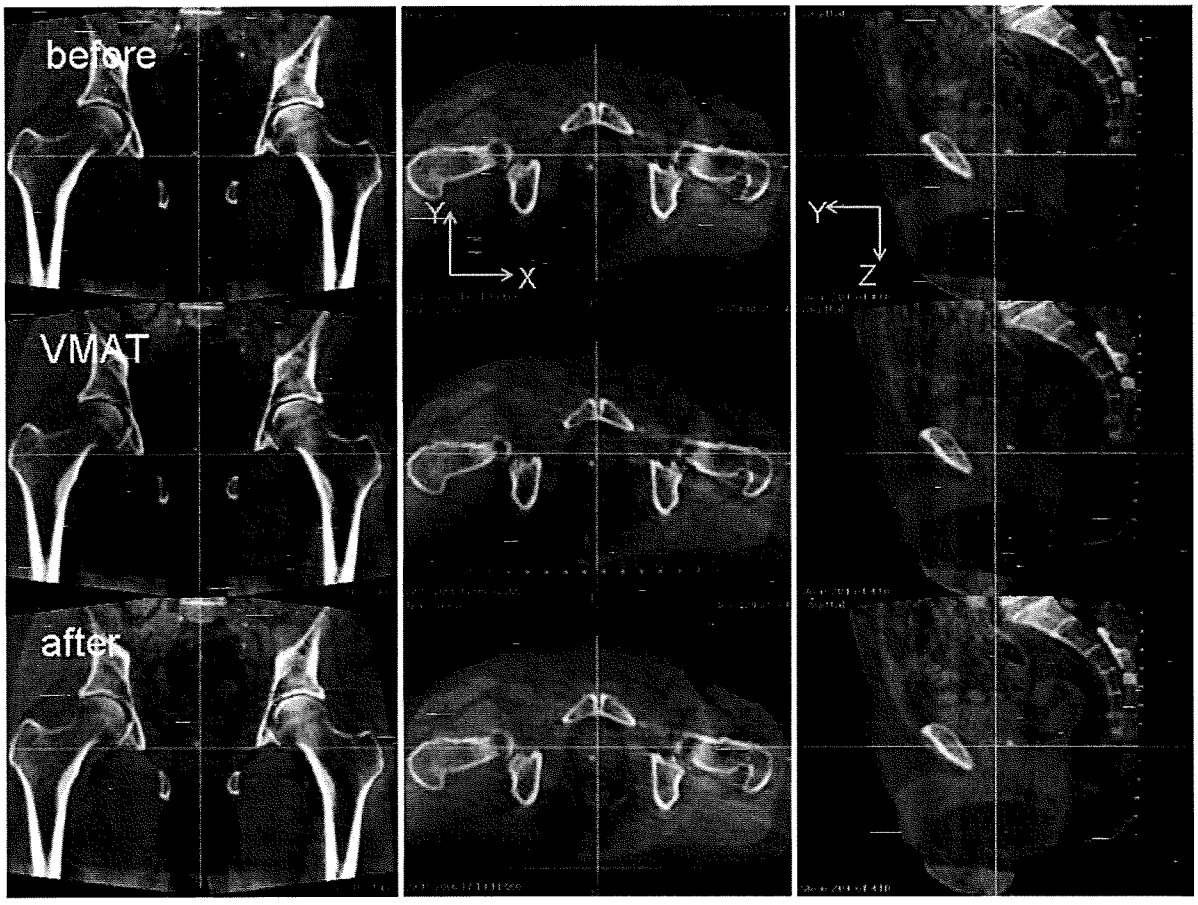

Figure 1. Cone-beam CT images of a prostate cancer patient with calcification inside the prostate organ. Images in the first row were acquired immediately before VMAT treatment after couch adjustment, the second row refers to images during VMAT delivery, and the third row images were taken immediately after the treatment. Crossing lines indicate the isocenter.

Declaration of interest: Dr. Nakagawa receives research funding from Elekta K.K.

References

[1] Nakagawa K, Haga A, Shiraishi K, Yamashita H, Igaki H, Terahara A, et al. First clinical cone-beam CT imaging during volumetric modulated arc therapy. Radiother Oncol 2009;90: 422–3.

[2] Williams P, Sykes J, Moore CJ. The effects of radiation scatter from simultaneous MV irradiation on kV fluoroscopic and x-ray volume imaging with the Elekta Synergy system, ESTRO, Amsterdam 2004. Radiother Oncol 2004;73 (Suppl 1).

[3] Nakagawa K, Yamashita H, Shiraishi K, Igaki H, Terahara A, Nakamura N, et al. Verification of in-treatment tumor position using kilovoltage cone-beam computed tomography: A preliminary study. Int J Radiat Oncol Biol Phys 2007;69: 970–3.

[4] Haskå TM, Honoré H, Muren LP, Høyer M, Pousen PR. Intrafraction changes of prostate position and geometrical errors studied by continuous electronic portal imaging. Acta Oncol 2008;47:1351–7.

Badminton, rectal cancer and 25 kg weight gain during chemotherapy

CHRISTIAN RIKLIN[1], DANIEL GUNTERN[2], SERGE LEYVRAZ[1] & MICHAEL MONTEMURRO[1]

[1]*Multidisciplinary Oncology Centre, University of Lausanne Hospitals (CHUV), Rue du Bugnon 46, CH-1011 Lausanne, Switzerland and* [2]*Radiology, University of Lausanne Hospitals (CHUV), Rue du Bugnon 46, CH-1011 Lausanne, Switzerland*

To the Editor

Chemotherapy is an integral part of today's multimodality cancer treatment. Side effects related to chemotherapy such as vomiting or weight loss are well known and treated routinely. Weight gain on the other hand is an often neglected problem although it has an important impact on both patient's quality of life and cancer prognosis. Analysis of the impressive weight gain in this case report clearly highlights the problem.

A 40-year-old premenopausal female patient in excellent general health was diagnosed in our institute in April 2006 with a locally advanced rectal cancer, cT4 cN1 cM0. The patient is a non-smoking, top female athlete and professional badminton teacher, who exercised three hours per day in addition to teaching badminton during the rest of the day. There was no incidence of weight changes before cancer diagnosis in our 162 cm tall patient. After establishing a protective colostomy neoadjuvant radiochemotherapy was started, during which the patient gained 2.7 kg body weight.

In June 2006, three weeks after radiochemotherapy, a pT4 pN1 tumor was successfully resected and adjuvant chemotherapy was started. In December 2006 the patient had gained another 12.5 kg body weight, when a seizure struck her. A CT scan showed left cerebral vein thrombosis of the inferior anastomotic vein of Labbé, the transverse sinus, the sigmoid sinus and the internal jugular vein. Extensive investigations did not identify any predisposing reason or underlying condition. Thus we concluded on a multifactorial origin; we hypothesized that chemotherapy-induced hypercoagulability, antiemetic steroid medication and the patient's physical inactivity likely induced a prothrombotic state. We suspected that the significant weight gain might in itself have also contributed to the thrombosis [1]. The patient was put on Valproate for seizure control and anticoagulated with low molecular heparin followed by acenocoumarol. Adjuvant chemotherapy was not reintroduced.

From start of treatment in April 2006 until October 2007 the patient's body weight increased from 61.8 kg to 87 kg, i.e. a total weight gain of 25.2 kg in 18 months. Being a top athlete, the patient had regular follow-up at the Swiss Accident Insurance Fund where her body composition was regularly monitored before, during and after treatment (Figure 1), indicating that weight gain was almost entirely due to an increase in body fat, amounting to at least 20.9 kg.

Correspondence: Michael Montemurro, Multidisciplinary Oncology Centre, University of Lausanne Hospitals (CHUV), Rue du Bugnon 46, CH-1011 Lausanne, Switzerland. Tel: +41 21 314 09 13. Fax: +41 21 314 02 00. E-mail: michael.montemurro@chuv.ch

(Received 10 March 2009; accepted 20 March 2009)

34-186X print/ISSN 1651-226X online © 2009 Informa UK Ltd. (Informa Healthcare, Taylor & Francis AS)
3109/02841860902913561

Acta Oncologica, 2009; 48: 1193–1197

informa
healthcare

ORIGINAL ARTICLE

Quality assurance of volumetric modulated arc therapy using Elekta Synergy

AKIHIRO HAGA[1], KEIICHI NAKAGAWA[1], KENSHIRO SHIRAISHI[1], SAORI ITOH[1], ATSURO TERAHARA[1], HIDEOMI YAMASHITA[1], KUNI OHTOMO[1], SHIGEKI SAEGUSA[1], TOSHIKAZU IMAE[1], KIYOSHI YODA[2] & ROBERTO PELLEGRINI[3]

[1]*Department of Radiology, University of Tokyo Hospital, 7-3-1 Hongo, Bunkyo-ku, Tokyo 113-8655 Japan,* [2]*Elekta KK, Kobe, Japan and* [3]*Elekta, 30 Line, Milano, Italy*

Abstract

Purpose. Recently, Elekta has supplied volumetric modulated arc therapy (VMAT) in which multi-leaf collimator (MLC) shape, jaw position, collimator angle, and gantry speed vary continuously during gantry rotation. A quality assurance procedure for VMAT delivery is described. *Methods and materials.* A single-arc VMAT plan with 73 control points (CPs) and 5-degree gantry angle spacing for a prostate cancer patient has been created by ERGO++ treatment planning system (TPS), where MLC shapes are given by anatomic relationship between a target and organs at risk and the monitor unit for each CP is optimized based on given dose prescriptions. Actual leaf and jaw positions, gantry angles and dose rates during prostate VMAT delivery were recorded in every 0.25 seconds, and the errors between planned and actual values were evaluated. The dose re-calculation using these recorded data has been performed and compared with the original TPS plan using the gamma index. *Results.* Typical peak errors of gantry angles, leaf positions, and jaw positions were 3 degrees, 0.6 mm, and 1 mm, respectively. The dose distribution obtained by the TPS plan and the recalculated one agreed well under 2%-2 mm gamma index criteria. *Conclusions.* Quality assurance for prostate VMAT delivery has been performed with a satisfied result.

The concept of volumetric modulated arc therapy (VMAT) originated from the conformal avoidance radiation therapy [1] with a dynamical movement of MLC while rotating the gantry. By modulating beam intensity during the gantry rotation, intensity modulated arc therapy (IMAT) was proposed and further investigated [2–6]. VMAT is one of the techniques to realize IMAT by varying gantry speed and dose rate with dynamical movement of MLC and jaw [7]. Recently, this has been clinically available [8–10] and a combination of Elekta Synergy with the latest linac control software and ERGO++ treatment planning system (TPS) is one example.

The purpose of this paper is to investigate how much error is caused in dose distribution due to the fluctuation in the dynamical parameters. The linac controller in Elekta Synergy (Elekta, Crawley, UK), RT Desktop 7.0.1, serves to record measured data of dose rates, gantry angles, MLC and jaw positions with 0.25 s interval during VMAT treatment. We can evaluate the influence of these errors by recalculating the dose distribution with these actual dynamical parameters. Since this is an independent simulation analysis and therefore we may be able to specify the cause when VMAT film verification failed.

Methods and materials

A single-arc VMAT plan for prostate cancer was created by ERGO++ v1.71 TPS (Elekta/3DLine, Milano) with D95 prescription (dose to 95% of target volume) of 76 Gy in 38 fractions. A single arc was discretized into 73 static beams or CPs placed at 5-degree gantry angle intervals between −175 and +175 degrees and the first and last CPs were positioned at −179 and +179 degrees (Figure 1). The field shape for each control point was determined by either conformal or conformal avoidance strategy with a 6 mm leaf margin to Planning Target Volume (PTV). In other words, the rectum was

Correspondence: Akihiro Haga, Department of Radiology, University of Tokyo Hospital, 7-3-1 Hongo, Bunkyo-ku, Tokyo 113-8655 Japan. Tel: +81 3 5800 9002. Fax: +81 3 5800 8786. E-mail: haga-haga@umin.ac.jp

(Received 5 April 2009; accepted 30 May 2009)

34-186X print/ISSN 1651-226X online © 2009 Informa UK Ltd. (Informa Healthcare, Taylor & Francis AS)
3109/02841860903081905

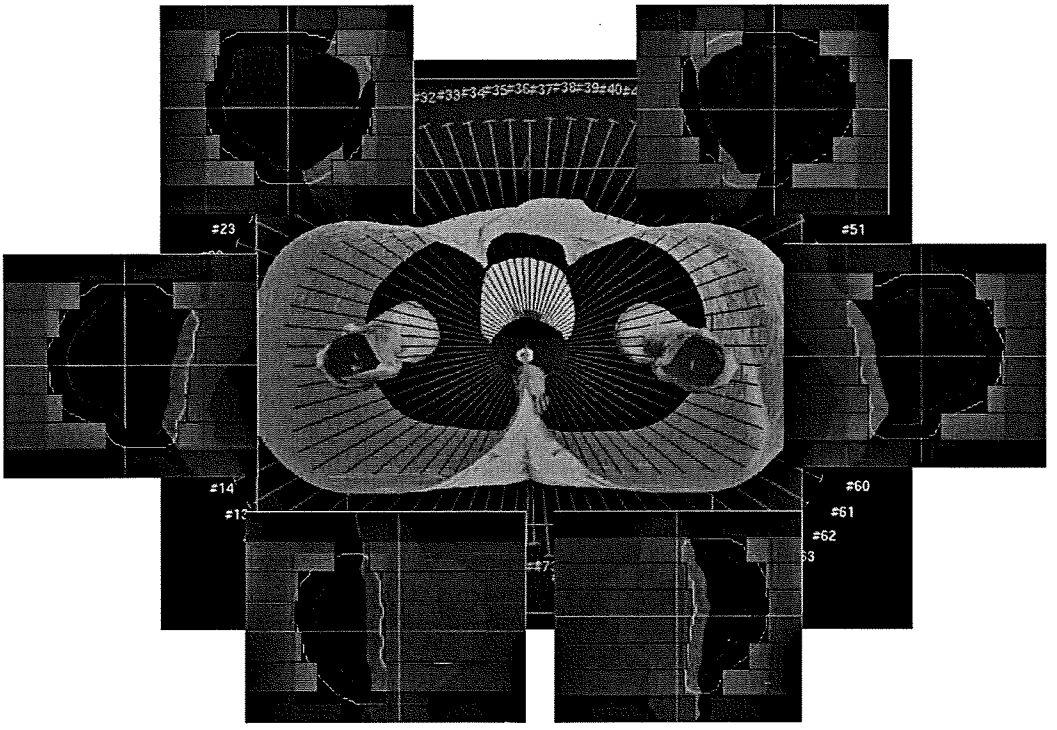

Figure 1. A single-arc VMAT plan with 73 CPs and 5-degree gantry angle spacing for a prostate cancer patient has been created by ERGO++ treatment planning system, where MLC shapes are given by anatomies of target and organs at risk and monitor units for each CP is optimized by simulated annealing algorithm based on given dose prescriptions. The red and pink regions are PTV and rectum, respectively.

partially shielded by MLC when it was in front of the target in beam's eye view, while the whole target was irradiated when it was in front of the rectum.

In the present study, the collimator angle was fixed at 180 degrees. Beam weights for all CPs were optimized by inverse planning based on the simulated annealing algorithm. Dose grid resolution was 2 mm × 2 mm × 2 mm for 3D calculation. After inverse planning, the CPs were grouped into a single arc with the VMAT sequencer in ERGO++ TPS, where a monitor unit (MU) to be delivered between two adjacent CPs was calculated by adding MUs at the two adjacent CPs and then multiplied by 0.5. The created plan was sent to MOSAIQ v1.6 (Elekta IMPAC, USA), and then delivered by the RT desktop controller.

For dose verification, VMAT plan was transferred to two phantom studies. One was a cylindrical water phantom with 0.015 cc pin-point ionization chamber (Type 31014, PTW, Germany) placed at the isocentre. The other was a pelvic water phantom including a GafChromic film (International Specialty Products, NJ, USA) to measure the dose distribution on axial, coronal, and sagittal planes including the isocentre. The GafChromic film was scanned using a flatbed scanner (EPSON GT-X770, Japan) and the gamma index with 3% of a dose at the measurement point and 3 mm has been evaluated by using DD-system v9.0 (R-tech, Japan).

The linac controller in service mode was capable of recording the actual gantry angle, MLC and jaw positions, and dose rate as a function of time. The MLC and jaw positions in each CP computed by ERGO++ were compared with the corresponding measured values. The cumulative MU error is practically negligible because Elekta VMAT delivery is based on MU-based servo control. Instead, the gantry angle error is discussed, which is defined as the difference between the gantry angle for each CP and the gantry angle where a cumulative MU reaches a specified value. A gantry speed dependence of these errors with the same VMAT plan was also examined by employing two times slower gantry speed than a commonly used clinical speed.

Using the actual data of gantry angle, MLC and jaw positions, and the cumulative MUs, dose distribution was re-calculated using Pinnacle v7.4i TPS (Philips, USA), and the dose in the original plan transferred into Pinnacle was compared with the re-calculated dose distribution.

Results

The beam-on time was typically 100 s for a single-arc prostate VMAT delivery. The isocentre dose discrepancy between plans and measurements for 17 patients was $-0.5 \pm 0.8\%$ (s.d.). The averages of the pass rate with a gamma criteria of 3 mm and 3% of a dose at the measurement point were 97.3%, 91.8%, and 92.2% on axial, sagittal, and coronal planes for a region having a dose greater than 30% of the isocentre dose, respectively.

Figure 2 demonstrates measured errors between planned and actual gantry angles during VMAT delivery for three consecutive runs. The red data points show the position errors for a normal delivery time of 100 s, whereas the blue data points show those for a delivery time of 200 s. The bar shows the error range for the three runs. The gantry angle ranges of zero gantry angle error were due to move-only control points with no dose delivery.

Figure 3a and b show measured errors between planned and actual leaf positions during VMAT delivery for three consecutive runs of the same VMAT plan as in Figure 2. Figure 3a depicts a position error of right leaf number 20, which is one of the centre leaves, whereas Figure 3b depicts a position error of left leaf number 20. Again the red data points show the position errors for a normal delivery time of 100 s, whereas the blue data points show those for a delivery time of 200 s. The bar shows the error range for the three runs. The gantry angle ranges of zero leaf error were due to move-only control points with no dose delivery.

Figure 4a and b depicts measured errors between planned and actual X1 and X2 back-up jaw positions, respectively, during VMAT delivery for three consecutive runs of the same VMAT plan. Once again, the red data points show the position errors for a normal delivery time of 100 s, whereas the blue data points show those for a delivery time of

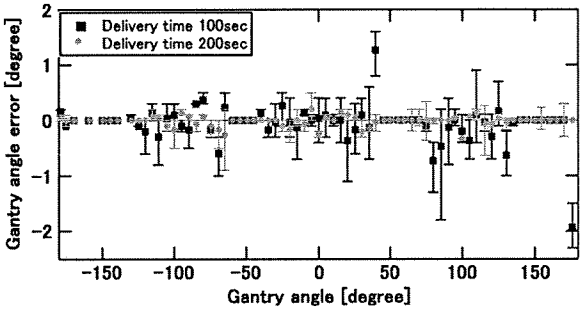

Figure 2. Measured errors between planned and actual gantry angles for three consecutive runs of the same VMAT plan. The red data points show the position errors for a normal delivery time of 100 s, whereas the blue data points show those for a delivery time of 200 s. The bar shows the error range for the three runs.

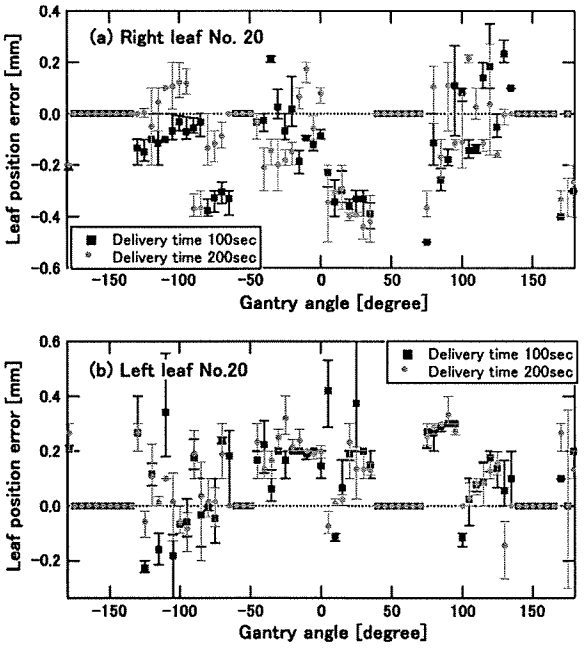

Figure 3. Measured errors between planned and actual leaf positions of the two centre leaves for three consecutive runs of the same VMAT plan: (a) position error of right leaf number 20, (b) position error of left leaf number 20. Again the red data points show the position errors for a normal delivery time of 100 s, whereas the blue data points show those for a delivery time of 200 s. The bar shows the error range for the three runs. The gantry angle ranges of zero leaf error were due to move-only control points with no dose delivery.

200 s. The bar shows the error range for the three runs. The gantry angle ranges of zero back-up jaw error were due to move-only control points with no dose delivery.

Figure 5a and b show gamma-index comparisons between an ERGO++ plan and re-calculated dose using actual data of MLC and jaw positions, gantry angles, and MUs with an interval of every 1 s. The red areas indicate gamma indices of larger than one under criteria of (a) 2% of a dose at the calculated point and 2 mm and (b) 1% of a dose at the calculated point and 1 mm.

Discussion

We have shown highly accurate prostate VMAT delivery using Elekta Synergy and ERGO++ TPS. While the dose agreement in the isocentre shows that total MU is correctly delivered, the agreement of dose distribution on axial, sagittal, and coronal planes assures accurate VMAT delivery. In the Synergy control system, the MLC, jaw, and gantry speed are servo-controlled based on cumulative MUs in each CP. Hence the errors in such dynamical parameters are quickly compensated by

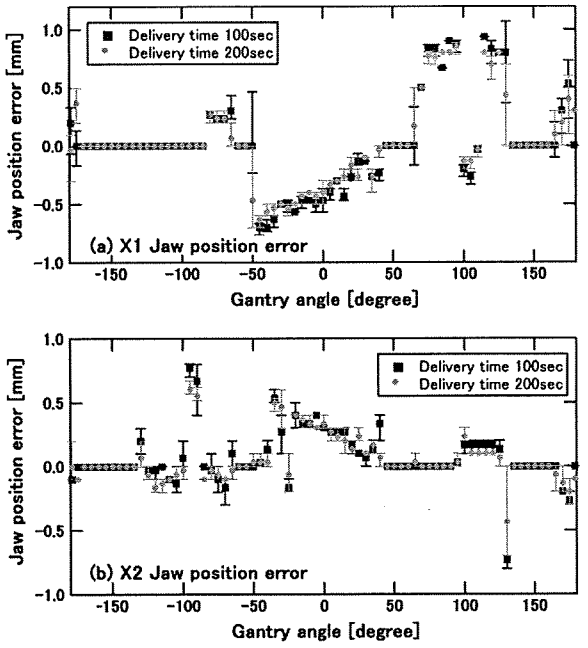

Figure 4. Measured errors between planned and actual back-up jaw positions for three consecutive runs of the same VMAT plan: (a) position error of X1 jaw, (b) position error of X2 jaw. Once again the red data points show the position errors for a normal delivery time of 100 s, whereas the blue data points show those for a delivery time of 200 s. The bar shows the error range for the three runs. The gantry angle ranges of zero back-up jaw error were due to move-only control points with no dose delivery.

real-time feedback control. For instance, it was found that the gantry angle error was immediately corrected as seen in Figure 2. In addition to the mechanical control, it is very important to mention that ERGO++ creates the MLC shape based on the anatomy relationship between the target and organs at risk from the beams eye view. Since it is a smooth function of gantry angle, no major changes are observed in MLC and jaw positions between adjacent control points thereby leading to more accurate dose calculation in TPS.

In the present work, the errors in gantry angles, MLC and jaw positions during VMAT delivery were analyzed. As seen in Figures 2–4, these errors were reproduced among three consecutive runs of the same VMAT plan, and were considered to be caused by accelerations of gantry, leaves, and jaws, which were required in almost the same gantry angles. In fact, it was clearly observed that the gantry angle error decreased when the gantry speed was slower as shown in Figure 2. In principle, smaller leaf and jaw position errors can be anticipated when the gantry speed is slower due to lower leaf and jaw speeds. In the present prostate plan which has no large leaf and jaw movements during gantry rotation, the leaf and back-up jaw position errors were comparable between two different delivery times. Instead, error tolerances of leaf and jaw positions given in the radiation control system may be a major cause of the observed errors.

As shown in Figure 5, the influence of these dynamical errors was negligible under criteria of 2% of a dose at the calculated point and 2 mm. Even under 1% of a dose at the calculated point and 1 mm criteria, the result was good except for low dose region. In other words, the errors in the dynamical parameters with the observed orders in prostate VMAT delivery do not affect the resulting dose distribution significantly.

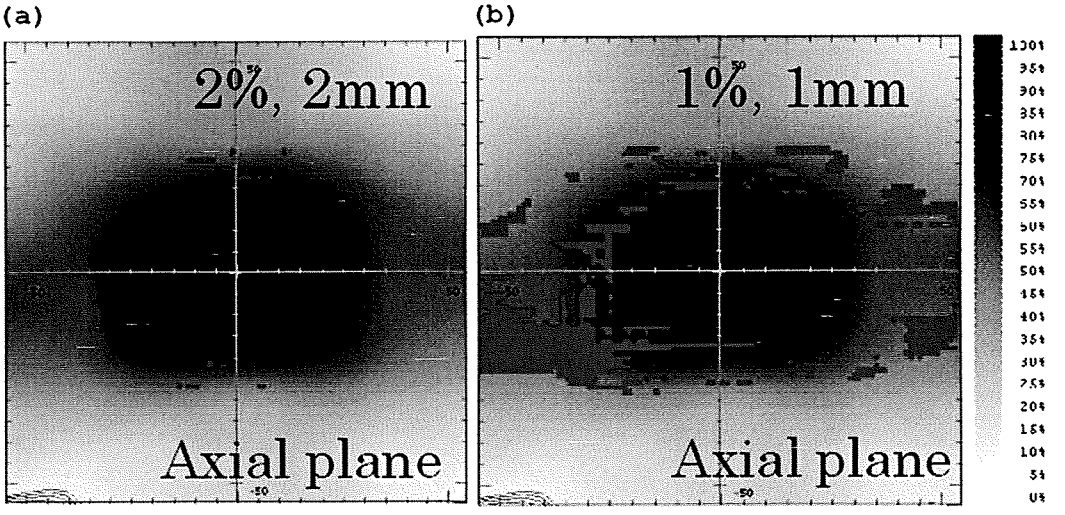

Figure 5. Gamma comparison between an ERGO++ plan and re-calculated dose using actual data of MLC and jaw positions, gantry angles, and MUs with an interval of every 1 s. The red areas indicate gamma indices of larger than one under criteria of (a) 2% of a dose at the calculated point and 2 mm and (b) 1% of a dose at the calculated point and 1 mm.

Conclusion

VMAT dose measurement for prostate cancer agreed well with the plan created by ERGO++. The observed errors of the dynamical parameter did not affect the dose distribution significantly. Quality assurance for prostate VMAT plans has been performed with a satisfied result.

Declaration of interest: Dr. Nakagawa receives research funding from Elekta KK.

References

[1] Takahashi S. Conformation radiotherapy: Rotation techniques as applied to radiography and radiotherapy of cancer. Acta Radiol Suppl 1965;242:1–142.

[2] Yu CX. Intensity-modulated arc therapy with dynamic multileaf collimation: An alternative to tomotherapy. Phys Mod Biol 1995;40:1435–49.

[3] Yu CX, Li XA, Ma I, et al. Clinical implementation of intensity modulated arc therapy. Int J Radiat Oncol Biol Phys 2002;53:453–6.

[4] Earl MA, Shepard DM, Maqvi SA, et al. Intensity modulated arc therapy simplified. Int J Radiat Oncol Biol Phys 2002;53:222–35.

[5] Earl MA, Shepard DM, Maqvi SA, et al. Inverse planning for intensity modulated arc therapy using direct aperture optimization. Phys Med Biol 2003;48:1075–89.

[6] Shepard DM, Cao D, Afghan MKN, Earl MA. An arc-sequencing algorithm for intensity modulated arc therapy. Med Phys 2007;34:464–70.

[7] Otto K. Volumetric modulated arc therapy: IMRT in a single gantry arc. Med Phys 2008;35:310–7.

[8] Bedford JL, Nordmark HV, MacNair HA, Aitken AH, Brock JE, et al. Treatment of lung cancer using volumetric modulated arc therapy and image guidance: A case study. Acta Oncol 2008;47:1438–43.

[9] Bedford JL, Warrington AP. Commissioning of volumetric modulated arc therapy (VMAT). Int J Radiat Oncol Biol Phys 2009;73:537–45.

[10] Korrenman S, Medin J, Kristoffersen FK. Dosimetric verification of RapidArc treatment delivery. Acta Oncol 2009;48:185–91.

Int. J. Radiation Oncology Biol. Phys., Vol. 75, No. 2, pp. 558–563, 2009

0360-3016/09/$–see front matter

ELSEVIER

doi:10.1016/j.ijrobp.2008.11.070

5TH JUCTS AND THE 5TH S. TAKAHASHI MEMORIAL INTERNATIONAL JOINT SYMPOSIUM

EFFECT OF AUDIO COACHING ON CORRELATION OF ABDOMINAL DISPLACEMENT WITH LUNG TUMOR MOTION

MITSUHIRO NAKAMURA, M.S.,* YUICHIRO NARITA, PH.D.,* YUKINORI MATSUO, M.D., PH.D.,* MASARU NARABAYASHI, M.D.,* MANABU NAKATA, R.T.T.,† AKIRA SAWADA, PH.D.,* TAKASHI MIZOWAKI, M.D., PH.D.,* YASUSHI NAGATA, M.D., PH.D.,‡ AND MASAHIRO HIRAOKA, M.D., PH.D.*

*Department of Radiation Oncology and Image-applied Therapy, Kyoto University Graduate School of Medicine, Kyoto, Japan; †Clinical Radiology Service Division, Kyoto University Hospital, Kyoto, Japan; and ‡Division of Radiation Oncology, Hiroshima University Hospital, Hiroshima, Japan

Purpose: To assess the effect of audio coaching on the time-dependent behavior of the correlation between abdominal motion and lung tumor motion and the corresponding lung tumor position mismatches.

Methods and Materials: Six patients who had a lung tumor with a motion range >8 mm were enrolled in the present study. Breathing-synchronized fluoroscopy was performed initially without audio coaching, followed by fluoroscopy with recorded audio coaching for multiple days. Two different measurements, anteroposterior abdominal displacement using the real-time positioning management system and superoinferior (SI) lung tumor motion by X-ray fluoroscopy, were performed simultaneously. Their sequential images were recorded using one display system. The lung tumor position was automatically detected with a template matching technique. The relationship between the abdominal and lung tumor motion was analyzed with and without audio coaching.

Results: The mean SI tumor displacement was 10.4 mm without audio coaching and increased to 23.0 mm with audio coaching ($p < .01$). The correlation coefficients ranged from 0.89 to 0.97 with free breathing. Applying audio coaching, the correlation coefficients improved significantly (range, 0.93–0.99; $p < .01$), and the SI lung tumor position mismatches became larger in 75% of all sessions.

Conclusion: Audio coaching served to increase the degree of correlation and make it more reproducible. In addition, the phase shifts between tumor motion and abdominal displacement were improved; however, all patients breathed more deeply, and the SI lung tumor position mismatches became slightly larger with audio coaching than without audio coaching. © 2009 Elsevier Inc.

Lung cancer, tumor motion, respiratory gated radiotherapy, audio coaching, correlation.

INTRODUCTION

During conventional radiotherapy (RT) planning for tumor movement with respiration, an internal margin is added around the clinical target volume to ensure complete coverage of the clinical target volume as it moves because of respiration within a treatment session (1). Therefore, it follows that a large amount of the surrounding normal tissue will be irradiated, increasing the amount of healthy tissue irradiated and limiting the maximal dose that can be prescribed to the tumor itself. An abdominal plate, called "diaphragm control (DC)," has been reported to be suitable for lung tumors to regulate respiratory motion (2). Although DC has been applied for patients during stereotactic body RT (SBRT) when the lung tumor motion was >8 mm at our institution, it was found that DC sometimes had little effect and was unusable because of poor respiratory function.

As techniques to explicitly account for respiratory-induced tumor movement, breath-hold (3–5), respiratory gated RT (6–10), and four-dimensional (11, 12) techniques are effective in reducing internal margin, resulting in a lower dose to the normal tissue and thus a lower risk of complications. Among these techniques, respiratory gated RT has been successfully applied to thorax and abdomen lesions in some institutions (6–10). During respiratory gated RT, the treatment device is periodically turned on and off, in phase or amplitude with the patient's breathing pattern, to restrict

Reprint requests to: Mitsuhiro Nakamura, M.S., Kyoto University Graduate School of Medicine, Kyoto, 54 Kawahara-cho, Shogoin, Sakyo-ku, Kyoto 606-8507 Japan. Tel: (+81) 75-751-3419; Fax: (+81) 75-771-9749; E-mail: m_nkmr@kuhp.kyoto-u.ac.jp

Supported in part by a Grant-in-Aid for Scientific Research from the Ministry of Education, Culture, Sports, Science and Technology of Japan (Grant 20229009).

Presented in part at the Fifth Japan-U.S. Cancer Therapy Symposium and the Fifth S. Takahashi Memorial International Joint Symposium, Sendai, Japan, September 7–9, 2007.

Conflict of interest: none.

Received Aug 27, 2008, and in revised form Nov 17, 2008. Accepted for publication Nov 22, 2008.

the range of tumor positions during dose delivery. Two types of gating methods have been categorized: internal and external gated RT. Internal gated RT accurately delivers a dose by monitoring the tumor position in real time using implanted fiducial markers (8). External gated RT requires the acquisition of a respiration surrogate signal to represent the tumor position (6, 7, 9, 10). Although external gated RT is less invasive for patients, the accuracy of the correlation depends on the stability of the tumor-surrogate phase or amplitude relationships during the treatment course.

In our institution, we are scheduled to perform external gated RT for patients who need DC during SBRT for lung cancer or advanced-stage lung cancer; however, we have been concerned about the correlation between the abdominal displacement and lung tumor motion in the superoinferior (SI) direction. Although Ahn *et al.* (13) and Hoisak *et al.* (14) reported a generally strong correlation without implanted fiducial markers, no guarantee exists that similar results have been obtained at our institution. Some researchers have also reported that the phase of organ motion does not necessarily match that of the surrogate motion (13–19). Phase shifts must be addressed to maintain the accuracy of the gating window. Ionascu *et al.* (17) used a real-time RT system and quantitatively estimated the time-dependent behavior of the correlation between abdominal displacement and implanted fiducial marker motion, and their corresponding amplitude mismatches. They suggested that it is necessary to increase the treatment margins to ensure the phase shifts.

The preliminary study for gated RT began under an institutional review board-approved protocol in May 2007. We developed an in-house method to investigate the tumor–abdominal motion relationship without implanted fiducial markers and showed a high correlation between these motions for 11 patients with lung cancer during free breathing (19). In addition, we have been planning to incorporate audio coaching to improve the efficiency of external gated RT for patients with an irregular breathing pattern (20, 21). Although Kini *et al.* (20) concluded that audio coaching improved the stability of respiration frequency, the effect of audio coaching on phase shifts and their corresponding lung tumor position mismatches have not yet been examined.

The purpose of the present study was to assess the effect of audio coaching on the correlations of abdominal displacement with lung tumor motion in the SI direction and the SI lung tumor position mismatches between abdominal displacement as a surrogate for the lung tumor position and the measured lung tumor position.

METHODS AND MATERIALS

Patients

Of the patients who underwent SBRT in four fractions for lung tumors between May 2007 and December 2007, 6 patients, who met following criteria, were enrolled in the present study: the lung tumor was clearly identified by X-ray fluoroscopy (Acuity, Varian Medical Systems, Palo Alto, CA) and the average peak-to-trough SI extent of the lung tumor displacement was >8 mm with X-ray fluoroscopy, as verified by several radiation oncologists. Of the 6 patients, 4 were men and 2 were women (median age, 78 years; range, 62–81). The lung tumors were located in the right middle lobe (n = 1), right lower lobe (n = 3), left upper lobe (n = 1), and left lower lobe (n = 1). The patient characteristics are listed in Table 1.

Data acquisition

A marker block with two infrared reflecting dots was placed on the anterior abdominal surface of the patient. The anteroposterior (AP) abdominal skin surface displacement was measured using the real-time positioning management system (Varian Medical Systems). The SI lung tumor motion was simultaneously acquired using X-ray fluoroscopy from the anterior of the patients. The X-ray fluoroscopy video signal was recorded at a frame rate of 30 Hz. The screen of the computer monitoring the abdominal displacement was displayed in parallel on the X-ray fluoroscopy console monitor using the remote desktop feature (maximal data transfer rate, 1 Gb/s) in Windows XP Professional so that the lung tumor motion and abdominal displacement were displayed on the same screen (Fig. 1). From the results of the preliminary verification, the phase error due to the signal delay of the local area network connection was sufficiently small (19).

All patients underwent an X-ray fluoroscopic examination of 60 s in duration with free breathing. They were then asked to breathe following simple audio coaching, such as "breathe in, breathe out," at a suitable tempo for each patient. They were trained for 5 min with the audio coaching to ensure they were comfortable with the breathing tempo and to make any adjustments necessary. After the breathing exercise, an X-ray fluoroscopic examination was performed again with audio coaching for 60 s. The X-ray fluoroscopy console monitor on which the abdominal displacement was simultaneously displayed was recorded on a digital video disk for each measurement. The measurements were performed at SBRT planning (Session 1), the second treatment session (Session 2), and at the end of treatment (Session 3). The interval between Sessions 1 and 3 was 10 days, and the duration of SBRT was within 1 week.

Tracking procedure and analysis

Custom software was developed by a medical physicist (M.N.) to automatically identify the lung tumor position to be detected on fluoroscopic images. The feasibility of our method for identifying the lung tumor position has been previously proved (19).

First, the software reads the recorded fluoroscopic images and runs the following procedure. A reflective marker position was detected using binary image processing and the mean AP abdominal displacement was then calculated. After measuring the reflective marker position, a rectangular region of interest (ROI) was set in the image that sufficiently contained the extent of lung tumor motion throughout the whole breathing cycle. A median filter with a 3 × 3 filter kernel was used to reduce the noise within the ROI. Image histograms within the ROI were equalized to enhance the contrast between the lung tumor and the background; thereafter, a template matching technique was applied to automatically detect the lung tumor. We have found that a basic single-template approach for lung tumor tracking does not work well for lung tumor tracking on X-ray fluoroscopic images because of the following tumor motion characteristics: the projected lung tumor shape and appearance vary more or less as a function of the breathing phase; and the X-ray fluoroscopic image intensities change with chest expansion and contraction. To reduce the false detection of the lung tumor position, three templates of the lung tumor for the exhale (end-ex), inhale

Table 1. Patient characteristics

Pt. No.	Age (y)	Gender	PS	Tumor location	Tumor size (mm)
1	78	Male	0	RLL	23
2	77	Male	1	RLL	20
3	62	Female	0	LLL	18
4	81	Male	0	LUL	29
5	77	Female	0	RLL	15
6	78	Male	0	RML	27

Abbreviations: Pt. No. = patient number; PS = performance status; RLL = right lower lobe; LLL = left lower lobe; LUL = left upper lobe; RML = right middle lobe.

(end-in), and middle (mid) respiratory phase were used. The method of difference measures ($D_k, k \in [end\text{-}in, end\text{-}ex, mid]$), based on the square of the difference between the templates and the background image, was defined as follows:

$$D_{end-in}(x,y) = \sum_{i=0}^{M-1}\sum_{j=0}^{N-1}\{f(x+i,y+j) - g_{end-in}(i,j)\}^2 \quad (1)$$

$$D_{end-ex}(x,y) = \sum_{i=0}^{M-1}\sum_{j=0}^{N-1}\{f(x+i,y+j) - g_{end-ex}(i,j)\}^2 \quad (2)$$

$$D_{mid}(x,y) = \sum_{i=0}^{M-1}\sum_{j=0}^{N-1}\{f(x+i,y+j) - g_{mid}(i,j)\}^2 \quad (3)$$

where N and M represent the length and width of the template, and $f(x, y)$ and $g_k(x, y)$, ($k \in [end\text{-}in, end\text{-}ex, mid]$) is the pixel intensity at location (x, y) of the ROI and templates, respectively. The region of minimal difference can be determined as the location of the lung tumor (x^*, y^*), as follows:

$$(x*, y*) = \arg\min_{(x,y)\in ROI}(D_{end-in}(x,y), D_{end-ex}(x,y), D_{mid}(x,y)) \quad (4)$$

The average displacement of lung tumor motion was measured according to the maximal peak-to-trough SI extent of the tumor displacement. To evaluate the tumor–abdominal phase relationship, the cross-correlation of the time-synchronized tumor–abdominal motion and its phase shifts was calculated. The SI lung tumor position mismatches between the predicted and measured lung tumor position were computed according to the method of Ionascu *et al.* (17). The mean value and 99% confidence interval of the SI lung tumor position mismatches were also calculated. The one-sided Wilcoxon test was performed for the statistical analyses. Values of $p < .01$ were regarded as significant.

RESULTS

Figure 2a,b illustrates the SI tumor displacement and AP abdominal displacement during the full respiratory cycle with and without audio coaching, respectively. The error bars represent the standard deviation (SD). The mean ± SD of tumor displacement was 10.4 ± 3.0 mm (range, 8.2–18.9) for patients during free breathing (FB). Audio coaching increased the displacement to a mean ± SD of 23.0 ± 11.6 mm (range, 10.1–46.2). The mean ± SD of abdominal displacement was 6.5 ± 2.2 mm for FB. These values increased to 17.3 ± 6.1 mm with audio coaching. A significant difference was observed between these groups in both displacements ($p < .01$).

Table 2 lists the correlation coefficients of tumor motion with abdominal displacement for each patient with and without audio coaching. The mean ± SD of the correlation coefficients was 0.95 ± 0.02 (range, 0.89–0.97) for FB. The maximal phase shift was 0.13 s for FB. The mean ± SD of the correlation coefficients was 0.97 ± 0.02 (range, 0.93–0.99) for audio coaching. The mean correlation coefficient between these groups was also significant ($p < .01$). Figure 3a,b shows a diagram of the lung tumor displacement vs. time and a scatterplot of the lung tumor displacement vs. abdominal displacement for Patient 5 in Session 3, respectively. Of all the patients, the greatest improvement in the correlation coefficient was observed for Patient 5. Using audio coaching, the average SI tumor displacement increased from 9.4 to 18.5 mm (Fig. 3a), and the observed phase shift between the tumor motion and abdominal displacement was reduced (Fig. 3b).

The SI lung tumor position mismatches for FB and audio coaching are summarized in Table 3. These mismatches persisted and varied daily. Although the SI lung tumor position mismatches became larger in 75% of all sessions with audio coaching compared with FB, no significant difference was observed between these groups ($p = .01$). The SI lung tumor position mismatches were within an average of 1.70 mm for FB and 2.09 mm for audio coaching.

DISCUSSION

Treatment planning and dose delivery of external gated RT requires intra- and interfraction reproducibility of the tumor–surrogate relationship (13, 14, 19) and stability of the intra- and interfraction target position (22) during the treatment course. In the present study, we evaluated the effect of audio

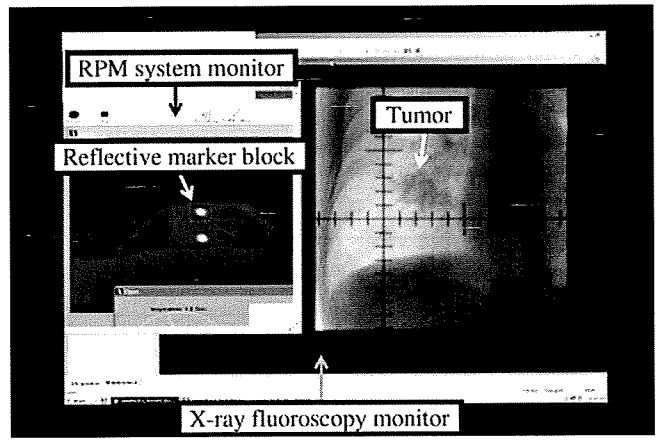

Fig. 1. Parallel display of real-time positioning management system monitor showing abdominal motion using reflective marker block and chest fluoroscopic image, which can project tumor shape from anterior of patient.

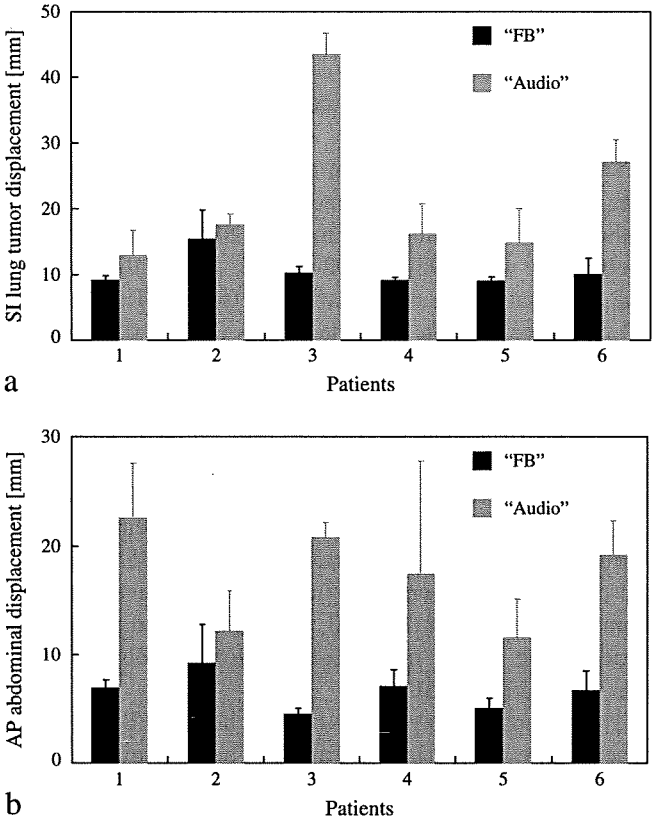

Fig. 2. (a) Superoinferior tumor displacement and (b) anteroposterior abdominal displacement averaged for consecutive respiratory cycles with and without audio coaching. Error bars show standard deviation.

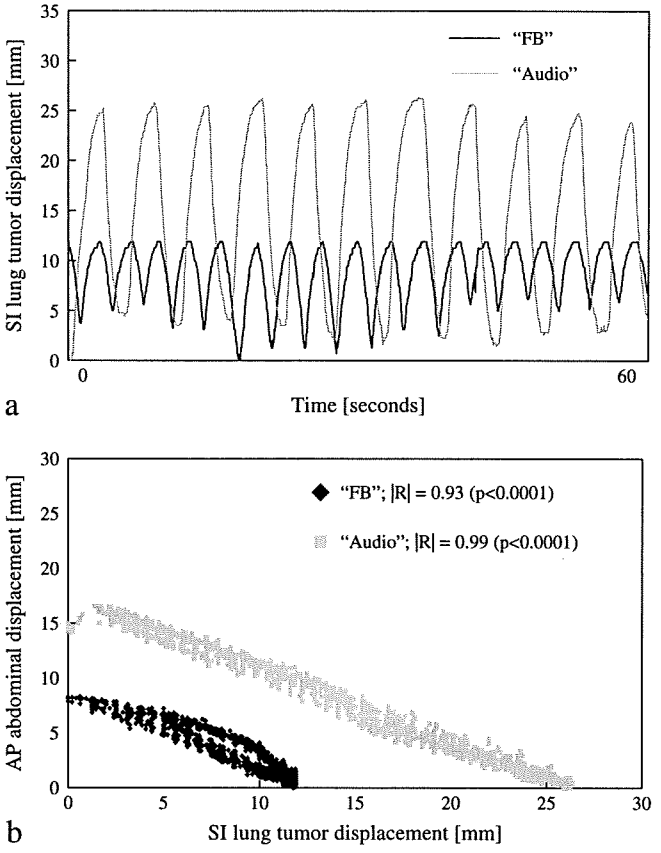

Fig. 3. (a) Time course of superoinferior lung tumor position and (b) scatterplot showing relationship with abdominal position for Patient 5 in Session 3, with and without audio coaching.

coaching on the correlation of abdominal displacement with lung tumor motion and SI lung tumor position mismatches using a template matching technique. Audio coaching generally led to an increase in the abdominal and lung tumor displacements in the AP and SI direction, respectively. Although a significant difference was shown in the tumor–abdominal correlation between the audio coaching and FB, the SI lung tumor position mismatches became slightly larger with audio coaching than without audio coaching.

A strong correlation between the external surrogate signals and internal tumor motion is required to perform external gated RT securely. Ahn *et al.* (13) used skin markers as the external surrogate signal and verified the relationship between the movement of the skin and the target organ. They showed a strong correlation (mean ± SD, 0.77 ± 0.12) between the skin and tumor movement, especially for sites in the lower lung. Hoisak *et al.* (14) assessed the correlation of abdominal displacement with the tumor motion as seen on X-ray fluoroscopy for multiple days, and reported a correlation range of 0.39–0.98. Because of the smaller phase shifts in our study than in their study, high correlation coefficients were obtained with FB. A possible cause of the phase shifts included the breathing type. Two main types of breathing exist: chest breathing and abdominal breathing. We estimated that the tumor and abdominal skin surface might move concurrently in abdominal breathing, which would result in reducing the phase shifts between the lung tumor and abdominal skin surface. In contrast, a slight time lag would occur between the abdominal skin surface and the lung tumor motion in chest breathing. If chest breathing is directed to abdominal breathing, external gated RT using an abdominal motion signal would then be performed more accurately because of the better tumor–abdominal correlation. In addition, patients tended to breathe consciously during audio coaching; thus, chest breathing might switch to abdominal breathing (23). The diaphragm is an important muscle and controls abdominal and lung tumor movement during respiration. Using audio coaching, the relaxation/contraction of the diaphragm might be stimulated. Thus, it is possible that

Table 2. Tumor–abdominal motion correlation coefficients throughout measurement sessions

	Free breathing			Audio coaching		
Pt. No.	Session 1	Session 2	Session 3	Session 1	Session 2	Session 3
1	0.97	0.97	0.97	NA	0.98	0.99
2	0.96	0.96	0.95	0.96	0.98	0.98
3	0.97	0.96	0.94	0.99	0.98	0.99
4	0.93	0.95	0.94	0.94	0.93	0.94
5	0.89	0.96	0.93	NA	0.99	0.99
6	0.93	0.97	0.97	0.95	0.96	0.97

Abbreviations: Pt. No. = patient number; NA = not available (patient did not participate in measurement session).

Table 3. Mean SI lung tumor position mismatches with and without audio coaching

	Free breathing (mm)			Audio coaching (mm)		
Pt. No.	Session 1	Session 2	Session 3	Session 1	Session 2	Session 3
1	0.49 (0.47–0.52)	0.71 (0.68–0.73)	0.61 (0.59–0.64)	NA	0.52 (0.49–0.54)	0.71 (0.67–0.75)
2	1.70 (1.63–1.77)	0.88 (0.85–0.92)	1.00 (0.95–1.06)	1.66 (1.58–1.74)	1.12 (1.08–1.17)	0.53 (0.50–0.55)
3	1.21 (1.15–1.26)	1.26 (1.18–1.33)	0.61 (0.58–0.64)	1.60 (1.51–1.69)	1.70 (1.60–1.79)	1.18 (1.13–1.24)
4	0.44 (0.42–0.46)	0.73 (0.70–0.76)	0.67 (0.64–0.70)	1.49 (1.40–1.57)	1.82 (1.74–1.89)	0.93 (0.89–0.97)
5	0.84 (0.80–0.88)	0.53 (0.50–0.55)	0.86 (0.86–0.90)	NA	0.57 (0.54–0.60)	0.69 (0.65–0.72)
6	0.77 (0.73–0.81)	0.45 (0.42–0.48)	0.69 (0.66–0.71)	1.30 (1.24–1.37)	1.72 (1.61–1.82)	2.09 (1.98–2.20)

Abbreviations: SI = superoinferior; other abbreviations as in Table 2.
Data in parentheses are 99% confidence intervals.

stimulation might have resulted in amplification of the lung tumor and abdominal displacement in the present study.

Although audio coaching significantly improved the tumor–abdominal motion correlation ($p < .01$), the total tumor movement as measured during the full respiratory cycle became larger, comparable with the results of Haasbeek *et al.* (24). Audio coaching not only stimulated tumor movement (Fig. 2a), but often resulted in a slight increase in the differences between the predicted and measured lung tumor position in the SI direction (Table 3). For example, the mismatch was an average of ≥1 mm for 62.5% of audio coaching compared with 22.2% of FB. Seppenwoolde *et al.* (25) used implanted fiducial markers and reported that the lung tumor moved with a degree of deviation from the mean trajectory position. Because the tumor largely moves during the respiration cycle, the deviation would be more pronounced. This would result in an increase in the SI lung tumor position mismatches. In contrast, audio coaching reduced the SI lung tumor position mismatches in 25% of the sessions. Thus, it was difficult to identify which factor, phase shift or tumor displacement, predominantly affected the SI lung tumor position mismatches in the present study. Additional margins or expansion of the gating window would be needed to compensate for these uncertainties in clinical practice.

An additional issue in external gated RT with audio coaching alone is an increase in the SI lung tumor position mismatches resulting from the larger motion range of the lung tumor. Haasbeek *et al.* (24) also concluded that differences in lung tumor position >5 mm between FB and audio coaching were detected in ≤56% of lung tumors with a motion range >10 mm (24). On the basis of our results, and theirs, it is more important to manage respiratory motion when applying audio coaching alone to external gated RT. As one of the methods to reduce SI lung tumor position mismatches, audiovisual biofeedback is expected to be suitable (26). The advantage of audiovisual biofeedback compared with audio coaching is that patients can maintain an arbitrary depth of respiration. Thus, it should result in a decrease in the mismatches between the predicted and measured lung tumor position.

CONCLUSION

Audio coaching served to increase the degree of correlation and made it more reproducible. In addition, the phase shifts between the tumor motion and abdominal displacement improved. All patients breathed more deeply, and the SI lung tumor position mismatches became slightly larger with audio coaching than without audio coaching.

REFERENCES

1. International Commission on Radiation Units and Measurements. Prescribing, recording and reporting photon beam therapy: Report No. 62 (supplement to ICRU report No. 50. Bethesda: ICRU; 1999.
2. Negoro Y, Nagata Y, Aoki T, *et al.* The effectiveness of an immobilization device in conformal radiotherapy for lung tumor: Reduction of respiratory tumor movement and evaluation of the daily setup accuracy. *Int J Radiat Oncol Biol Phys* 2001; 50:889–898.
3. Hanley J, Debois MM, Mah D, *et al.* Deep inspiration breath-hold technique for lung tumors: The potential value of target immobilization reduced lung density in dose escalation. *Int J Radiat Oncol Biol Phys* 1999;45:603–611.
4. Rosenzweig KE, Hanley J, Mah D, *et al.* The deep inspiration breath-hold technique in the treatment of inoperable non small-cell lung cancer. *Int J Radiat Oncol Biol Phys* 2000;48: 81–87.
5. Mah D, Hanley J, Rosenzweig KE, *et al.* Technical aspects of the deep inspiration breath-hold technique in the treatment of thoracic cancer. *Int J Radiat Oncol Biol Phys* 2000;48: 1175–1185.
6. Ramsey CR, Cordrey IL, Oliver AL. A comparison of beam characteristics for gated and nongated clinical x-ray beams. *Med Phys* 1999;26:2086–2091.
7. Paoli J, Rosenzweig KE, Yorke E, *et al.* Comparison of different respiratory levels in the treatment of lung cancer: Implications for gated treatment. *Int J Radiat Oncol Biol Phys* 1999;45: 386–387.
8. Shirato H, Shimizu S, Kunieda T, *et al.* Physical aspects of a real-time tracking system for gated radiotherapy. *Int J Radiat Oncol Biol Phys* 2000;48:1187–1195.
9. Ford EC, Mageras GS, Yorke E, *et al.* Evaluation of respiratory movement during gated radiotherapy using film and electronic portal imaging. *Int J Radiat Oncol Biol Phys* 2002;52:522–531.
10. Berson AM, Emery R, Rodriguez L, *et al.* Clinical experience using respiratory gated radiation therapy: Comparison of free-breathing and breath-hold techniques. *Int J Radiat Oncol Biol Phys* 2004;60:419–426.

11. Keall PJ, Kini V, Vedam SS, *et al.* Motion adaptive X-ray therapy: A feasibility study. *Phys Med Biol* 2001;46:1–10.
12. Keall PJ, Joshi S, Vedam SS, *et al.* Four-dimensional radiotherapy planning for DMLC-based respiratory motion tracking. *Med Phys* 2005;32:942–951.
13. Ahn S, Yi B, Suh Y, *et al.* A feasibility study on the prediction of tumour location in the lung from skin motion. *Br J Radiol* 2004;77:588–596.
14. Hoisak JD, Sixel KE, Tirona R, *et al.* Correlation of lung tumor motion with external surrogate indicators of respiration. *Int J Radiat Oncol Biol Phys* 2004;60:1298–1306.
15. Vedam SS, Keall PJ, Kini V, *et al.* Determining parameters for respiratory gated radiotherapy. *Med Phys* 2001;28:2139–2146.
16. Ozhasoglu C, Murphy MJ. Issues in respiratory motion compensation during external-beam radiotherapy. *Int J Radiat Oncol Biol Phys* 2002;52:1389–1399.
17. Ionascu D, Jiang SB, Nishioka S, *et al.* Internal-external correlation investigations of respiratory induced motion of lung tumors. *Med Phys* 2007;34:3893–3903.
18. Mageras GS, Yorke ED, Rosenzweig A, *et al.* Fluoroscopic evaluation of diaphragmatic motion reduction with a respiratory gated radiotherapy system. *J Appl Clin Med Phys* 2001;2: 191–200.
19. Nakamura M, Narita Y, Matsuo Y, *et al.* Correlative analysis of abdominal motion with lung tumor motion for non-invasive respiratory gated radiotherapy. *J Jpn Soc Ther Radiol Oncol* 2008;20:119–125.
20. Kini VR, Vedam SS, Keall PJ, *et al.* Patient training in respiratory-gated radiotherapy. *Med Dosim* 2003;28:7–11.
21. Kubo HD, Wang L. Introduction of audio gating to further reduce organ motion in breathing synchronized radiotherapy. *Med Phys* 2002;29:345–350.
22. Juhler NT, Korreman SS, Pedersen AN, *et al.* Intra- and interfraction breathing variations during curative radiotherapy for lung cancer. *Radiother Oncol* 2007;84:40–48.
23. Neicu T, Berbeco R, Wolfgang J, *et al.* Synchronized moving aperture radiation therapy (SMART): Improvement of breathing pattern reproducibility using respiratory coaching. *Phys Med Biol* 2006;51:617–636.
24. Haasbeek CJA, Spoelstra FOB, Lagerwaard FJ, *et al.* Impact of audio-coaching on the position of lung tumors. *Int J Radiat Oncol Biol Phys* 2008;71:1118–1123.
25. Seppenwoolde Y, Shirato H, Kitamura K, *et al.* Precise and real-time measurement of 3D tumor motion in lung due to breathing and heartbeat, measured during radiotherapy. *Int J Radiat Oncol Biol Phys* 2002;53:822–834.
26. George R, Chung TD, Vedam SS, *et al.* Audio-visual biofeedback for respiratory-gated radiotherapy: Impact of audio coaching and audio-visual biofeedback on respiratory-gated radiotherapy. *Int J Radiat Oncol Biol Phys* 2006;65:924–933.

Int. J. Radiation Oncology Biol. Phys., Vol. 75, No. 2, pp. 369–377, 2009

0360-3016/09/$–see front matter

ELSEVIER

doi:10.1016/j.ijrobp.2009.02.081

5TH JUCTS AND THE 5TH S. TAKAHASHI MEMORIAL INTERNATIONAL JOINT SYMPOSIUM

INTRA-ARTERIAL INFUSION CHEMOTHERAPY USING CISPLATIN WITH RADIOTHERAPY FOR STAGE III SQUAMOUS CELL CARCINOMA OF THE CERVIX

YUKO KANEYASU, M.D., PH.D.,* NOBUTAKA NAGAI, M.D., PH.D.,† YASUSHI NAGATA, M.D., PH.D.,* YASUTOSHI HASHIMOTO, M.D.,* SHINTARO YUKI, M.D.,* YUJI MURAKAMI, M.D., PH.D.,* MASAHIRO KENJO, M.D.,* HIDEAKI KAKIZAWA, M.D., PH.D.,§ NAOYUKI TOYOTA, M.D., PH.D.,§ HISAYA FUJIWARA, M.D., PH.D.,‖ YOSHIKI KUDO, M.D., PH.D.,‖ AND KATSUHIDE ITO, M.D., PH.D.§

*Department of Radiation Oncology, Graduate School of Biomedical Sciences, Hiroshima University, Hiroshima, Japan; †Department of Obstetrics and Gynecology, Asa Citizen Hospital, Hiroshima, Japan; §Graduate School of Biomedical Sciences, Department of Radiology, Graduate School of Biomedical Sciences, Hiroshima University, Hiroshima, Japan; and ‖Department of Obstetrics and Gynecology, Hiroshima University, Hiroshima, Japan

Purpose: To examine the effectiveness of concomitant intra-arterial infusion chemotherapy (IAIC) using cisplatin (CDDP) with radiotherapy for Stage III squamous cell carcinoma of the cervix.

Materials and Methods: We analyzed 29 cases of Stage III squamous cell carcinoma of the uterine cervix treated with radiotherapy and IAIC of CDDP from 1991 to 2006. External-beam therapy was given to the whole pelvis using four opposing parallel fields with an 18-MV linear accelerator unit. A central shield was used after 30–40 Gy with external whole-pelvic irradiation, and the total dose was 50 Gy. High-dose-rate brachytherapy was given with ^{192}Ir microSelectron. The dose at Point A was 6 Gy per fraction, 2 fractions per week, and the total number of fractions was either 3 or 4. Two or three courses of IAIC were given concomitantly with CDDP 120 mg or carboplatin 300 mg.

Results: We confirmed excellent medicine distribution directly by using computed tomographic angiography. The 5-year overall survival rate for Stage III patients was 62%, the cause-specific survival rate was 70%, and the local relapse-free survival rate was 89%. Local recurrence, distant metastasis, and occurrences of both were 7%, 38%, and 3%, respectively. The incidence of severe acute hematologic adverse reactions (Grade ≥3) was 27% for all patients; however, all recovered without interruption of radiotherapy. Severe nonhematologic effects (Grade ≥3) were 3%, including nausea and ileus. Only 1 patient's radiotherapy was interrupted for a period of 1 week because of ileus. Severe late complication rates (Grade ≥3) for the bladder, rectum, and intestine were 3%, 3%, and 10%, respectively.

Conclusion: A combination of IAIC and systemic chemotherapy should be considered to improve the prognosis of patients with Stage III squamous cell carcinoma of the cervix. © 2009 Elsevier Inc.

Cervical carcinoma, Intra-arterial infusion chemotherapy, Radiotherapy, High-dose-rate brachytherapy.

INTRODUCTION

Radical radiotherapy (RT) for patients with uterine cervical cancer is well established, and equally good treatment results have been obtained compared with early-stage surgical treatment. However, the prognosis for patients with advanced uterine cervical cancer is still poor. To improve the prognosis for patients with advanced cervical cancer, further effort is required. Since 1999 many investigators have started paying attention to platinum-based concurrent chemoradiotherapy (CCRT) (1–11), since the National Cancer Institute announced its recommendation of CCRT for cervical cancer, based on the treatment results of five randomized trials (12–16). However, there are some differences between the West and Japan in treatment policy: in the West, patient age for CCRT is approximately in the 40s (median), younger than Japanese patients, who are approximately in their 60s. In addition, patients with early-stage (IB–IIB) cancer receive CCRT in Europe and America, whereas they receive surgery in Japan. The above-mentioned studies (1–16) exhibit evidence of the effectiveness of CCRT in patients with early-stage (IB–IIB) cervical cancer, whereas no obvious evidence of survival benefit has been shown for patients with locally advanced cervical cancer.

Reprint requests to: Yuko Kaneyasu, M.D., Ph.D., Department of Radiation Oncology, Graduate School of Biomedical School Sciences, Hiroshima University, 1-2-3 Kasumi, Minamiku, Hiroshima 734-8551, Japan. Tel: (+81) 82-257-5257; Fax: (+81) 82-257-5259; E-mail: kaneyasu@hiroshima-u.ac.jp

Presented at the 5th Japan/US Cancer Therapy Symposium and the 5th Takahashi Memorial Joint Symposium, September 7–9, 2007, Sendai, Japan.

Conflict of interest: none.

Received Dec 3, 2008, and in revised form Feb 12, 2009. Accepted for publication Feb 12, 2009.

Intra-arterial infusion chemotherapy (IAIC) is considered useful for improvement of local control and survival, and many investigators have an interest in the use of neoadjuvant chemotherapy before radical surgery or RT and in the use of concurrent chemoradiotherapy (17–38). Many investigations have shown encouraging results for local control, but many reports have shown no definite effect on survival. There have been few reports on IAIC combined with concurrent RT. Moreover, there have been few reports concerning the evaluation of drug distribution.

We investigated the effect of concurrent IAIC with radical RT for advanced (Stage III) squamous cell carcinoma of the cervix. We have previously reported our experience with locally advanced (Stage II or higher) cervical cancer treated with this strategy (36). In this study we confirmed whether the anticancer drug had satisfactorily entered the tumor. Drug distribution was evaluated with computed tomographic angiography (angio-CT), and the drug was shown to be evenly distributed throughout the tumor.

We limited the cases to Stage III squamous cell carcinoma only, added patients treated between 1999 and 2006, and analyzed the long-term outcome for patients treated with concurrent IAIC and RT.

METHODS AND MATERIALS

Patients

Twenty-nine patients with Stage III squamous cell carcinoma of the cervix who were treated by RT and IAIC using cisplatin (CDDP) with curative intent at Hiroshima University from 1991 to 2006 were evaluated. The tumor was staged according to International Federation of Gynecology and Obstetrics criteria, and all patients were confirmed as Stage III. Two patents had Stage IIIA disease, and 27 patients had Stage IIIB disease. We excluded patients with obvious para-aortic lymph node (PAN) metastasis by CT at initial diagnosis. Patients were initially evaluated and staged by physical and pelvic examination by gynecologists and radiation oncologists, without general anesthesia.

Patient characteristics are shown in Table 1. Mean patient age was 56 years (range, 26–72 years). Stage III tumors were classified into three sizes: small (tumor slightly extending to the pelvic wall), medium (tumor massively extending to one pelvic wall), and large (tumor extending to both pelvic walls) (39). The number of patients with a small tumor was 1, with medium was 16, and with large was 12. There were 9 patients with keratinizing type, 19 with non–keratinizing type, and 1 with a further different type. Pelvic lymph node swelling was diagnosed by CT, and a clinically positive node was defined as a lymph node with a minimum diameter of >1 cm on CT. There were 7 patients with mild coexisting illness (*e.g.*, hypertension, diabetes mellitus). Previous abdominal surgery had been carried out in 9 patients.

Treatment policies

Our treatment policies are listed in Table 2. To decrease patient discomfort at application, our rate of whole-pelvic external irradiation was higher; however, our rate of intracavitary irradiation was lower than that of the Japanese general rules for clinical and pathologic management of uterine cervical cancer (39). We used IAIC for locally advanced cervical cancer.

Table 1. Patient characteristics

Patients	29
Age (y), mean (range)	56 (26–72)
Stage III tumor size*	
Small	1
Medium	16
Large	12
Histology	
Keratinizing	9
Nonkeratinizing	19
Other	1
Lymphadenopathy	
Yes	7
No	22
Coexisting illness (*e.g.*, diabetes mellitus, hypertension)	
Yes	7
No	22
Previous abdominal surgery (*e.g.*, appendectomy)	
Yes	9
No	20

Values are number except where noted.

* Small tumor (S): tumor slightly extending to the pelvic wall; medium tumor (M): tumor massively extending to one pelvic wall; large tumor (L): tumor extending to both pelvic walls.

Radiotherapy

External-beam RT (EBRT) was given to the whole pelvis using the parallel–opposed (anteroposterior–posteroanterior) technique or the four-field box technique with an 18-MV linear accelerator unit. The daily fraction size was 1.8–2 Gy, with 5 fractions weekly. The superior border of the anteroposterior–posteroanterior fields was the superior edge of L5, the inferior border was the obturator foramen, and fields extended laterally to 1.5–2 cm outside of the true pelvis. The anterior border of the lateral fields was over the anterior edge of the pubic symphysis, and the posterior border was the anterior surface of the sacrum. A central shield was used after 30–40 Gy (mean, 36.4 Gy) with external whole-pelvic irradiation, and the total dose was 50 Gy (mean, 50 Gy). High-dose-rate intracavitary brachytherapy was given with ^{192}Ir micro-Selectron for 27 patients. The dose at Point A was 6 Gy per fraction, 1 or 2 fractions per week, and the number of fractions was 3 or 4. Mean total dose of high-dose-rate intracavitary brachytherapy was 20.4 Gy (range, 12–30 Gy). For 2 patients, low-dose-rate intracavitary brachytherapy was

Table 2. Radiotherapy treatment policies

	External irradiation (Gy)		
Stage	Whole pelvis	Central shield	Intracavitary irradiation (Point A [Gy])/fractions)
I	0–30	45–50	18–30/3–5
II			
Small	0–30	45–50	18–30/3–5
Large	24–36	14–26	18–24/3–4
III			
Small–medium*	30–36	14–16	18/3
Large*	34–40	10–14	12–24/2–4
IVA*	36–50	0–14	12–24/2–4

Stage III tumor sizes as defined in Table 1 footnote.

* With chemotherapy (including intra-arterial infusion) where possible.